A sutible model for drying kenitic of wood fiber using halogen moistuer analayzer

Mohammad Arabi (marabi@uoz.ac.ir)
University of Zabol, Iran
Mohammad Dahmardeh Ghalehno
University of Zabol, Iran

Research Article

Keywords: Wood fiber, Drying kenitic, Moisture content, Artifical neural network

Posted Date: July 27th, 2022

DOI: https://doi.org/10.21203/rs.3.rs-1770600/v2

Abstract

Drying wood fiber is a complex, dynamic, highly nonlinear, and energy-intensive process involving simultaneous heat and mass transfer. So, the theoretical modeling of wood fiber drying because wood fiber shrinks anisotropically during a drying process is very complicated. The semi-theoretical and empirical thin-layer drying models developed on a laboratory scale are a suitable option for examining the drying kinetics of lignocellulose materials. In this study, drying kinetics of wood fibers were evaluated using 18 semi-empirical models at three temperatures of 105 °C, 120 °C, and 135 °C, utilizing a halogen moisture analyzer. The findings revealed that raising the temperature increased the drying constant while decreasing the drying time of wood fibers. According to drying curves, no constant drying rate was observed and all the drying process occurred in two falling drying rate periods. More specifically, despite the high initial moisture content of wood fiber about 170% (based on dry weight), the wood fiber drying process was mainly controlled by diffusion mechanism. The fitness of drying curves on semi-theoretical and empirical models based on statistical parameters, including root mean square error (RMSE), sum of square errors (SSE), and coefficient of determination (R2) showed that the Midilli et al. model had the highest coefficient of determination and the lowest error percentage. Also, the moisture content was more accurately predicted by ANN model than the Midilli et al. model.

Introduction

Wood cellulose fiber is the most abundant natural material on earth (Zhao et al. 2021). Cellulosic fibers have various uses due to their renewability, recyclability, and biodegradability, including textiles, papermaking, bio-based composites, polymer composites, and fiber-reinforced composites (Thyavilli et al. 2019). Adjusting moisture content in wood fiber through the drying period is a critical part of most wood product manufacturing processes. Due to their high strength and affordable cost, wood fibers are commonly used to reinforce wood-plastic composites (WPC) (Huang et al. 2006). Several studies have examined the effect of the drying process on the quality of wood fibers, their dispersion in the plastic matrix, and the mechanical characteristics of WPC (Huang et al. 2006; Chen et al. 2017). Accordingly, as water evaporates in natural fibers, pores form during the mixing of wood and polymer fibers, resulting in poor performance of wood-plastic composites (WPC). Therefore, natural fibers should be dried to about 1 % to 5 % before the mixing process (Huang et al. 2006). Drying cellulose fibers is a key step in the manufacturing process of medium-density fiberboard (MDF). In this regard, the moisture content of the fibers should be decreased to 8 to 12 % (based on dry weight) before pressing the fiber mat (Pang 2000). Lindell and Stenstrom (2006) reported that the dryer section consumes much energy (more than 80%) in paper mills. When utilizing biomass as fuel, the high moisture content of the biomass affects the combustion strongly. For example, the calorific value of dried biomass is 3.5 MW h/ton, while wet biomass is 2.2 MW h/ton (Rajendran 2017; Soni 2007). As aforementioned, drying wood and cellulose fibers consumes significant energy in all related applications, and it significantly impacts the ultimate pricing of products (Konopka et al. 2021). As a result, researchers and industry owners have always considered strategies to recognize and manage the drying process of wood and cellulose fibers. Modeling

the drying process of cellulose fibers is one technique to manage and identify the drying process. Several investigations have been carried out to simulate and examine the drying kinetic of wood and cellulosic fibers based on Fick's law of diffusion (Fernando et al. 2018; Chanpet et al. 2020; Autengruber et al. 2020; Remond et al. 2005; Winberg et al. 2000; Salin 2008; Dincer 1998). Recently, several studies have shown that the theoretical models do not adequately describe the fundamental aspects of the experimental wood drying process. Remond et al (2005) indicated that when softwoods dry, a thin and dry shell without free water develops quickly in the substrate near the wood surface, slowing the drying process and releasing free water from the substrates. These substrates are still saturated with free water. It has been shown by Wiberg and Moren (1999) that at the beginning of the drying process with high moisture content, the moisture content in the central part of Sapwood decreases very rapidly without any moisture gradients. The diffusion phenomenon cannot describe the moisture migration process gradient-free.

So, it is clear that when surface moisture evaporates quickly, the surface of the fibers also dries quickly, resulting in the highest wood shrinkage. Moreover, the diameter of pores in the wood cell wall will be decreased. Consequently, moisture cannot be transferred from the lower layers near the surface to the fiber surface (Li and Zhao 2020). Some researchers believe that some of the interactions and relationships between water and wood during the drying process at the microstructural scale are still unknown. (Penttila et al. 2021; Zitting et al.2021). As a result, mathematical modeling of the drying process of wood and cellulose fibers seems to be complex (Sander et al 2007). Due to shrinkage and deformation in the cell walls of wood fibers during the drying process, the accuracy of the presented mathematical models is questioned. The drying process of lignocellulosic materials, agricultural products, and food has been modeled using semi-empirical and experimental models (Verma et al 1985; Babalis et al 2006; Demir et al 2007; Doymaz 2007a; Gan and Pe. 2014). Fick's second law and its variants, as well as Newton's law of cooling, are used to develop experimental and semi-empirical models. They were primarily designed based on actual data collected in laboratory settings. Additionally, they are less complicated and more accessible to comprehend than mathematical models (Wang and Singh 1976; Hii et al 2009; Kumar et al 2012). Also, these models have shown a strong capacity to estimate and forecast the drying kinetics of various materials (Ertekin and Firat 2017; Midili et al. 2002). Thin drying layer modeling is one of the most effective approaches for analyzing the drying kinetics of hygroscopic materials (Ademiluyi et al 2008; Kaleta et al 2013). Thin-layer drying means to dry as one layer of sample particles or slices. It is assumed that there are the same air velocity and temperature throughout this thin layer. (Kaur and Singh 2014; Lee and Kim 2009; Vega et al. 2007). The drying kinetics of bacterial cellulose (Jatmiko et al 2017), Cotton fibers (Ghazanfari et al, 2006), and unbleached Kraft pulp sheet (Kong et al 2020) have all been investigated using thin-layer drying models, with promising findings.

Artificial neural network is one of the newest techniques for modeling and forecasting complex dynamic systems such as the wood drying process. Some researchers have utilized the ANNs to simulate the drying process of wood and agricultural products (Dash et al. 2020; Chai et al. 2019; Saxena et al. 2022). The neural network models have been utilized to simulate agricultural product drying kinetics as well as the wood drying process. Previous research has shown that the artificial neural network (ANN) is more

advantageous since it can precisely predict the drying kinetics and be easily applicable to non-linear processes. (Saxena et al. 2018).

Previous studies have employed conventional and convective dryers to study the drying kinetics of wood particles and cellulose fibers (Bry's et al. 2020; Arabi et al. 2017; Zarea Hosseinabadi et al. 2012). These drying methods involve several drawbacks, including low energy efficiency and lengthy drying time, especially in falling drying rate periods (Wang et al. 2007). Radiant dryers, such as halogens lamps, deliver heat to the material more quickly than convective or conductive dryers. As a result, the drying time decreases. The halogen hygrometer is a cutting-edge, quick, and precise method for detecting the moisture content of various materials. Halogen hygrometers are now acknowledged as a scientific, accurate approach and ASTM-accepted method in the industry (determination moisture of plastic granules by loss in weight in designation D6980-12). This is the first study to use a halogen hygrometer to describe the drying kinetics of wood fiber analysis. As a result, the research aims to explore the impact of halogen drying temperature on kinetic drying of wood fiber and predict the moisture content of wood fibers vs. time using artificial neural networks and thin drying layer models.

Materials And Method

Wood fibers were obtained from Arian Sina factory. In order to investigate the drying rate of wood fibers above the FSP point, they were combined with water in equal weight ratios for 24 hours and then stored in a sealed polyethylene bag at 3 ° C to 5 ° C for seven days. The sample was mixed every day to ensure that the wood fibers had a consistent moisture level. Finally, wood fibers with a moisture content of 170% (based on dry weight) were subjected to the drying process.

Drying process

Moisture Analyzer Halogen model MB45, manufactured by OHAUS, was used to dry wood fibers at three different temperatures: 105 ° C, 120 ° C, and 135 ° C. The MB45 has a sample capacity of 45g, with a readability of 0.001g and repeatability of 0.015% (using a 10g sample). The heater type of MB45 is a halogen lamp, and the operating temperature range is 50º C to 200º C in 1º C increments. The sample was heated in halogen hygrometers by absorbing the IR radiation produced by the halogen lamp. The weight difference before and after drying was used to determine the mass and moisture content of the sample continuously throughout the drying process. Halogen hygrometers work on the Loss on Drying (LOD) principle like oven dryers. However, there are various benefits such as quick drying time, ease of use, and direct measurement without computations compared to the oven dryer. To investigate the drying kinetics of wood fibers, 4 g of wet fibers were dispersed on a stainless steel tray placed on a precise and sensitive scale in the dryer compartment. The fiber was distributed on a tray carefully to prevent the fibers from accumulating at one point. After adjusting the temperature of the dryer chamber in the scope of this study, the weight loss values of the samples at a specified time interval, every 30 seconds, were presented and recorded online on the hygrometer display. The wood fibers continued to dry until the sample's moisture content was nearly zero. The tests were performed three times for each temperature, and the

mean moisture content measurements were used to design and fit the drying curves for each temperature.

Drying kinetics of wood fibers

The moisture content of wood fibers was measured according to Equations 1 and 2.

$$MR = \left(\frac{M_t - M_e}{M_0 - M_e}\right) \quad 1$$

$$MR = \left(\frac{M_{t+dt}}{M_0}\right) \quad 2$$

Where MR is the moisture ratio (dimensionless), M_t is the moisture content at time t (kg of solids/kg of water), M_e is the equilibrium moisture (kg of solids/kg of water), and M_0 is the initial moisture content (kg of solids/kg of water).

It should be noted that due to the insignificant value of M_e in comparison with Mt and M0, it can be saved. Therefore Eq. 1 can be simplified to Eq 2. (Ertekin and Firat 2017; Doymaz 2007a).

The drying rate of wood fibers was measured using Equation 3 (Ertekin and Firat 2017).

$$DR = \left(\frac{M_{t+dt} - M_t}{dt}\right) \quad 3$$

Where M_t and M_{t+dt} are the MC at t and MC at t+dt (kg moisture/kg dry matter), respectively, t is drying time (s). Equation 2 was used to obtain the moisture ratio of wood fibers at each temperature. Then, the experimental drying data of moisture ratio versus time was fitted to thin drying layer models using MATLAB 2016 software (Table 2). The models listed in Table 2 have already been widely used to investigate the drying kinetics of food, agricultural products, and municipal waste. The performance of these models was examined through comparing the coefficient of determination (R^2), sum squares of error (SSE), and root mean squared error (RMSE) which were calculated in relation to 4 to 6, respectively. The best thin drying layer model is the one with the smallest error value and the greatest coefficient of determination.

$$R^2 = \frac{\sum_{i=1}^{N}(MR_{exp,i} - \overline{MR}_{exp})(MR_{pre,i} - \overline{MR}_{pre})}{\sqrt{\left[\sum_{i=1}^{N}(MR_{exp,i} - \overline{MR}_{exp})^2\right]\left[\sum(MR_{pre,i} - \overline{MR}_{pre})^2\right]}} \quad (4)$$

$$RMSE = \left[\frac{1}{N}\sum_{I=1}^{n}(M_{pre,i} - M_{expi})\right]^{1/2} \quad (5)$$

$$SSE = \sum_{i=1}^{n}(MR_{pre,i} - MR_{exp})^2 \quad (6)$$

Where MR_{prei} and MR_{expi} are the predicted and experimental moisture ratios (MR) at i_{th} observation, respectively. MR_{exp} is the mean value of the explanatory variable, N is the number of observations, and n is the number of model parameters

Artificial Neural network model

Artificial neural network (ANN), as a nonlinear modeling method, is generally used to model complex physical phenomena such as the drying process of wood and lignocellulosic materials. The ANN configuration used in this study was a Multi-layer perceptron (MLP) consisting of one input layer, one or two hidden layers, and one output layer, as shown in Fig.1. The general form of the MLP output can be expressed mathematically in equation 7.

$$Y = g\left(\theta + \sum_{j=1}^{m} v_j\left[\sum_{i=1}^{n} f(W_{ij}X_i + \beta_j\right]\right) \quad (7)$$

Where Y is the prediction value of the dependent variable; X_i is the input value of ith independent variable; W_{ij} is the weight of the relationship between the ith input neuron and jth hidden neuron; βj is the bias value of the jth hidden neuron; vj is the weight of the relationship between the j_{th} hidden neuron and output neuron; θ is the bias value of output neuron; g (.) and f (.) are the activation functions of output and hidden neurons, respectively (Saxena et al. 2022). The input variables in the input layer were temperature, and drying time and the output variables in the output layer were moisture ratio. For ANN model building, the input data is split into 3 sets: training (70 %), testing (15 %), and validation (15 %). The number of the hidden layer and the number of neurons in these layers were determined by trial and error. The neural network was trained using the Levenberg-Marquardt (LM) learning algorithm. The transfer function of the hidden layer and output layer were hyperbolic tangent sigmoid and linear, respectively. The hyperbolic tangent sigmoid transfer function was as follows:

$$f(x) = \frac{2}{1 + e^{(-2x)}} - 1 \quad (8)$$

Where f (x) and x are the output and input values of neurons, respectively.

The coefficient of determination (R^2), mean squared error (MSE), and mean absolute error (MAE) were used to predict the ANN performance. Equations 9 to 11 include the formulas for computing these statistical characteristics.

$$MAPE = \frac{1}{n}\sum_{i=1}^{n}\left(\frac{|y_{exp.} - y_{pred.}|}{y_{exp.}}\right)100 \quad (9)$$

$$MSE = \frac{1}{n}\sum_{i=1}^{n}(y_{exp.} - y_{pred.})^2 \quad (10)$$

$$R^2 = 1 - \frac{\sum_{i=1}^{n}(y_{exp.} - y_{pred.})^2}{\sum_{i=1}^{n}(y_{exp.} - \overline{y_{exp.}})^2} \quad (11)$$

Where y exp is the actual data values, y pred is the predicted data values, is the average of the actual values, and n is the number of data.

Results And Discussion

Drying curves

Fig. 3. depicts the drying behavior of wood fibers using a moisture analyzer at 105 °C, 120 °C, and 130 °C. Accordingly, reaching the moisture content of wood fibers from 170 % (based on dry weight) to final moisture content (near zero) took 18, 14, and 12 minutes for 105 °C, 120 °C, and 135 ° C, respectively. As shown in Figure 3, the increase in the drying temperatures significantly decreased the drying times. In halogen moisture analyzer ohaus MB Series, the halogen radiator emits infrared radiation (IR) in the short wavelength range of 0.75–1.5 micrometers (near-infrared). When the halogen lamp is radiated toward the product, it is extremely heated and its thermal gradient within the material significantly increases in a short period. Since the halogen radiant energy can be easily passed through the air without heating the ambient air, this energy just heats the product. Thus, the internal part of materials would be warmer than the surrounding air and the rate of heat transfer is greater as compared to the hot air drying technique (Younis et al. 2018; Hung et al. 2021).Therfore, IR drying technology has the advantages of high energy efficiency, short drying time, uniform heating of materials, and low energy costs (Hung et al. 2021). The changes in drying rates versus drying time are shown in Fig. 4. Accordingly, the drying rate increased with an increase in drying temperature. Also, the drying speed was quick at the beginning of the drying operation (especially at a higher temperature), but the drying rate was slow by passing the time. It is due to a lack of sufficient moisture at the end point of the drying process. The relationship between drying rate and moisture content at different drying temperatures is shown in Fig. 5. Accordingly, the three drying periods were observed, including preheating period (A) and the first and second drying rate periods (B and

C). The constant drying rate period was not found; however, the initial moisture content of wood fibers was about 170% (based on dry weight). The morphological structure of fibers and drying techniques can significantly affect the drying process. When wood fibers are heated quickly by a moisture analyzer, many morphological changes might occur in their structures. The microstructure and rheological behaviour of the wood cell wall is closely intertwined with its moisture properties. Since, external layers of wood fibers are rapidly shrink, First of all, a thin and dry shell was formed near the surface of fibers that it create many barriers for migration moisture from internal layers to ones. (Li and Zhao 2020). Due to these morphological interactions, even if there is a lot of free water in the bottom layers, the rate of migration of water molecules from the interior to the surface is less than the rate of vaporization from the surface into the environment. Therefore, it is extremely difficult to find a constant drying rate period during the drying process of wood fibers. For lignocellulosic materials, constant drying rate periods are often extremely short or not seen at all (Kong et al. 2020; Arabi et al. 2017; Zarea Hosseinabadi et al. 2012). The heat and mass transfer in the drying process of solid material can be defined based on bio number (Sander et al. 2010). The constant drying is observed for solid materials with a bio number less than 0.1, while the bio number value for lignocellulosic materials was reported as more than 0.2 (Soni 2007). It means that the drying process and mass transfer parameters for biomass materials were mostly controlled by internal resistance (Dincer 1998). According to Fig 5, the drying process almost completely occurred in the first and second falling rate periods (B and C). The first falling drying rate happened when wet spots on the surface gradually diminished until the whole surface was dried. As a result, the surface moisture of the fibers decreased over time while the surface temperature increased. During this period, the drying process was controlled by moisture diffusion and internal resistances inside wood fibers. When the surface was totally dried, the second falling drying rate started at point C, and the dry surface was transmitted to the layers underneath the surface. According to Fig 5, about 60% of the total drying time occurred during this period. In this phase, the drying rate was independent of drying conditions such as temperature and moisture content. The moisture transfer might be due to liquid diffusion, capillary movement, and vapor diffusion. Also, the drying time was usually greater than the first falling drying rate period.

Drying curves fitting

The nonlinear regression approach and MATLAB 2016 software was used to fit moisture content data at various drying temperatures to the thin-layer drying models presented in Table 2. The regression constants (a, b, c, d...,), the drying constants (k), and the statistical indicators (R2, SSE, and RMSE) of the thin-layer drying models are shown in tables 3, 4, and 5 for 105 °C, 120 °C, and 135°C, respectively. Accordingly, The Midilli et al 2002 model showed the best fitting performance for describing kinetic drying of wood fibers at temperatures ranging from 90°C to 120°C (Tables 2,3, and 4). The Midilli et al. model is composed of an exponential and a linear term describing the moisture ratio as a function of drying time (Ertekin and Firat 2017). It successfully predicted the drying characteristics of poplar wood particles (Zarea Hosseinabadi, 2012) and cassava pulp (Charmongkolpradit and Luampon 2017).

ANN model

A multilayer perceptron consisting of layers with one or more neurons with different activation functions was employed to optimize the perceptron network. MLP model was developed based on temperature and drying time as input variables and moisture content as an output variable. The number of neurons in the hidden layer is variable (x). Experimental data were separated into three groups for the artificial neural network modeling, including training (70%), validation (15%), and testing (15%). After training and testing the network, the findings revealed that topology 2-5-1 with hyperbolic tangent sigmoid transfer functions provided the greatest training for content moisture modeling. The R values for MR for neural network training, validation, and testing data are shown in Fig. 6. In the training, validation, and testing data, as well as the total data, the R-values for MR were 0.99956, 0.99979, 0.99947, and 0.99958, respectively. According to Table 5, the total data in the artificial neural network for MR prediction had an absolute mean percent error (MAPE) of 2.53%. The artificial neural network showed a higher capacity to predict the moisture content of wood fibers than regression and thin-layer drying models, as evidenced by the high coefficient of determination and low error percentage between experimental and predicted data. Fig.7. depicts experimental data against predicted data obtained based on ANN models. Accordingly, the neural network predicted the experimental data (R^2) more accurately than Midilli et al, model. Artificial neural networks are unique machine learning algorithms that mimic the human brain and find the relationship between the data sets. Therefore, ANN can learn from the past data and improve its performance based on previous experience and training. Also, the designed program can adapt to new conditions in case of data change. These two factors of generalizability and adaptability distinguish the artificial neural network from other modeling methods and allow it to provide better results than other modeling methods. Many researchers have utilized ANNs to predict the drying process of wood and lignocellulosic materials. These studies employed MAPE, MSE, and R2 statistical parameters as the main comparison between experimental and predicted data. The findings from the current study are consistent with results from previous studies (Saxena et al. 2022). Overfitting is the most common issue in neural network training. This issue occurs when a neural network only performs well on training data and does not provide good results for other data sets. A periodic epoch performance chart for a neural network is shown in figure 8, when the error due to the validation data stays constant for six consecutive epochs, the neural network computation stops. As shown in Fig 8, after 25 epochs, the error was fixed in the following six consecutive periods, and the forecasting and data processing was stopped. This showed the network has been well-trained, validated, and tested.

Conclusion

The wood fibers are stretched during the drying process. This makes the wood fibers shrink more, creating small cracks in wood fibers. Moreover, moisture outlets will be blocked. As a result, applying mathematical models to analyze the drying kinetics of hygroscopic materials is complicated and challenging. Thin-layer drying of materials is a valuable tool for understanding the fundamental mechanism of moisture transport in hygroscopic materials since they are based on laboratory settings. Therefore, it is important to explore the thin-layer modeling approach for estimating the drying kinetics of wood fiber at 105 ° C, 120 ° C, and 135 ° C. The drying process was carried out with a halogen moisture

analyzer. A moisture analyzer is a device that determines the moisture content with the loss on drying method and consists of a weighing and halogen heating unit. The results showed that the drying constant increased with increasing temperature while the drying time of wood fibers decreased. Despite the high moisture content of wood fibers, about 170% db. (above FSP), the constant drying rate period was not observed during the drying period, and the whole drying process took place at a falling drying rate period. The performance of thin drying layer models was investigated based on statistical parameters including R2, SSE, and RMSE. The findings showed the Midili et al, 2002 model presented the best fit for the drying processes of the wood fibers. Moreover, the ANN model was more productive and precise than thin-layer drying methods for predicting changes in the moisture content of wood fibers. The results showed a moisture analyzer is a reliable tool for predicting moisture changes and drying kinetic of lignocellulose materials. As a result, as an innovative, rapid, and accurate approach, halogen radiation can be used to assess the quantity of moisture content and analyze the drying kinetics of lignocellulosic materials, particularly in MDF and particleboard manufacturing process.

Declarations

Ethical Approval: This article does not contain any studies with human participants or animals performed by any of the authors.

Consent to Participate: Authors consent to their participation in the entire review process.

Consent for Publication: Authors allow publication if the research is accepted.

Data Availability Statements: The datasets generated during and/or analysed during the current study are available from the corresponding author on reasonable request.

Competing Interests: The authors have no relevant financial or non-financial interests to disclose.

Funding: This work was supported by University of Zabol, Zabol, Iran. (Grant Number PR-UOZ1400-12).

Author Contributions: All authors contributed to the study conception and design. Material preparation, data collection and analysis were performed by Mohammad Arabi and Mohammad Dahmardeh Ghalehno. The first draft of the manuscript was written by Mohammad Arabi and all authors commented on previous versions of the manuscript. All authors read and approved the final manuscript.

Acknowledgements: We are grateful for financial support from the University of Zabol Grant Number (PR-UOZ1400-12).

Author Statements: The authors certify that they have participated sufficiently in the work to take public responsibility for the content. Furthermore, each author certifies that this material or similar material has not been and will not be submitted to or published in any other publication before its appearance in the Mechanics of Time-Dependent Materials journal.

References

1. Ademiluyi, T., Oboho, EO, Owudogu, M.: Investigation into the thin layer drying models of Nigerian popcorn varieties. Leonardo Electronic Journal of Practices and Technologies 13: 47–62. (2008)
2. Arabi, M., Faezipour, M., Layeghi, M., Khanali, M., Hosseinabadi, Z.: Evaluation of Thin-Layer models for Describing Drying Kinetics of Poplar Wood Particles in a Fluidized Bed Dryer.Particulat science and technology. 35(6)723–730. (2017) https://doi.org/10.1080/02726351 .2016 .11 96 275.
3. Autengruber, M., Lukacevic, M., Füssl, J.: Finite-element-based moisture transport model for wood including free water above the fiber saturation point. International Journal of Heat and Mass Transfer, 161, p.120228. (2020) https://doi.org/10.1016/j.ijheatmasstransfer.2020.120228.
4. Babalis, S.J., Papanicolaou, E., Kyriakis, N.: Evaluation of thin-layer drying models for describing drying kinetics of figs (Ficus carica). Journal of Food Engineering 75: 205–214. (2006) https://doi.org/10.1016/j.jfoodeng.2005.04.008.
5. Brys, A., Kaleta, A., Górnicki, K., Głowacki, S., Tulej, W., Bry´ J, Wichowski, P.: Some Aspects of the Modelling of Thin-Layer Drying of Sawdust. Energies. 14, 726. (2021) https://DOI: 10.3390 /en 14030726.
6. Charmongkolpradit, S., Luampon, R.: Study of thin layer drying model for cassava pulp. Energy Procedia, 138, 354–359. (2017) https://doi.org/10.1016/j.egypro.2017.10.138.
7. Chanpet, M., Rakmak, N., Matan, N., Siripatana, C.: Effect of air velocity, temperature, and relative humidity on drying kinetics of rubberwood. Heliyon, 6(10), p.e05151. (2020) https://doi.org/10.1016/j.heliyon.2020.e05151
8. Chen, F., Li, Q., Gao, X., Han, G., Cheng, W.: Impulse-cyclone drying treatment of poplar wood fibers and its effect on composite material's properties. BioResources, 12(2), 3948–3964. (2017) https://doi:10.15376/biores.12.2.3948-3964.
9. Chai, H., Chen, X., Cai, Y., Zhao, J.: Artificial neural network modeling for predicting wood moisture content in high frequency vacuum drying process. Forests, 10(1), p.16. (2019) https://doi:10.3390/f10010016.
10. Dash, K.K., Chakraborty, S., Singh, Y.R.: Modeling of microwave vacuum drying kinetics of bael (Aegle marmelos L.) pulp by using artificial neural network. Journal of the Institution of Engineers (India): Series A, pp.1–9. (2020) https://doi:10.1007/s40030-020-00431-x.
11. Demir, V., Gunhan, T., Yagcioglu, A.K.: Mathematical modelling of convection drying of green table olives. Biosystems Engineering 98: 47–53. (2007) https://doi.org/10.1016/j.biosystemseng .2007.06.011.
12. Dincer, I.: Moisture loss from wood products during drying—Part I: Moisture diffusivities and moisture transfer coefficients. Energy Sources, 20(1), 67–75. (1998) https://doi.org/10.1080/00908 319808970044.
13. Doymaz, I.: Air-drying characteristics of tomatoes. Journal of Food Engineering 78: 1291–1297. https://doi.org/10.1016/j.jfoodeng.2005.12.047. (2007a)

14. Fernando, N., Narayana, M., Wickramaarachchi, WAMKP.: The effects of air velocity, temperature and particle size on low-temperature bed drying of wood chips. Biomass Conversion and Biorefinery, 8(1), pp.211–223. (2018) https://doi:10.1007/s13399-017-0257-7.
15. Gan, P.L., Poh, P.E.: Investigation on the effect of shapes on the drying kinetics and sensory evaluation study of dried jackfruit. Intl J Sci Engr7:193–8. (2014) https://doi:10.12777/ijse.7.2.193-198.
16. Ghazanfari, A., Emami, S., Tabil, L.G ., Panigrahi, S .: Thin-layer drying of flax fiber: II. Modeling drying process using semi-theoretical and empirical models. Drying Technology, 24 (12), 1637–1642. (2006) https://doi.org/10.1080/07373930601031463.
17. Hii, C.L., Law, C.L., Cloke, M.: Modeling using a new thin layer drying model and product quality of cocoa. Journal of Food Engineering 90: 191–198. (2009) https://doi.org/10.1016/j.jfoodeng. 2008.06.022.
18. Huang, D., Yang. P., Tang, X., Luo, L., Sunden, B.: Application of infrared radiation in the drying of food products. Trends in Food Science & Technology.110:765 – 77. (2021) https://doi.Org/10.1016/j.tifs.2021.02.039.
19. Huang, S.H, Cortes, P., Cantwell., W.J. : The influence of moisture on the mechanical properties of wood polymer composites. Journal of materials science, 41(16), 5386–5390. (2006) https://doi:10.1007/s10853-006-0377-0.
20. Jatmiko, T.H., Rosyida, V.T., Indrianingsih, A.W., Apriyana, W.: Thin Layer Drying Model of Bacterial Cellulose Film. In IOP Conference Series: Earth and Environmental Science. 101(1). (2017) https://doi:10.1088/1755-1315/101/1/012011.
21. Kaleta, A., Gornicki, K.: Evaluation of drying models of apple (var. McIntosh) dried in a convective dryer. International Journal of Food Science and Technology 45: 891–898. (2010) https://doi:10.1111/j.1365-2621.2010.02230.x.
22. Kaleta, A., Górnicki, K., Winiczenko, R., Chojnacka, A.: Evaluation of drying models of apple (var. Ligol) dried in a fluidized bed dryer. Energy Convers. Manag, 67, 179–185. (2013) https://doi.org/10.1016/j.enconman.2012.11.011.
23. Kaur, K., Singh, A.K.: Drying kinetics and quality characteristics of beetroot slices under hot air followed by microwave finish drying. Afr J Agric Res 9(12):1036–44. (2014) https://doi:10.5897/AJAR2013.7759.
24. Kong, L., Yang, X., Hou, Z., Dong, J.: Mathematical modeling of drying kinetics for pulp sheet based on Fick's second law of diffusion. Journal of Korea TAPPI. 52(2), 23–31. (2020) https://doi:10.7584/JKTAPPI.2020.04.52.2.23
25. Kumar, N., Sarkar, B.C., Sharma, H.K.: Mathematical modeling of thin layer hot air drying of carrot pomace. Journal of Food Science and Technology 49: 33–41. (2012) https://doi:10.1007/s13197-011-0266-7.
26. Konopka, A., Barański, J., Orłowski, K.A., Mikielewicz, D., Dzurenda, L.: Mathematical model of the energy consumption calculation during the pine sawn wood (Pinus sylvestris L.) drying process.

Wood Science and Technology, 55(3), 741–755. (2021) https://doi:10.1007/s00226-021-01276-8.

27. Lindell, K., Stenström, S.: A modular process modeling tool for the analysis of energy use and cost in the pulp and paper industry. Drying Technology, 24(11), 1335–1345. (2006) https://doi.org/10.1080/07373930600951109.
28. Li, X., Zhao, Z.: Time domain-NMR studies of average pore size of wood cell walls during drying and moisture adsorption. Wood Science and Technology, 54(5), 1241–1251. (2020) https://doi.org/10.1007/s00226-020-01209-x.
29. Lee, J. H., Kim, H. J.: Vacuum drying kinetics of Asian white radish (raphanus sativus l.) slices. LWT-Food Science and Technology 42:180–186. (2009) https://doi.org/10.1016/j.lwt.2008. 05.017.
30. Midilli, A., Kucuk, H., Yapar, Z.: A new model for single-layer drying. Drying Technology 20: 1503–1513. (2002) https://doi.org/10.1081/DRT-120005864.
31. Pang, S.: Mathematical modelling of MDF fibre drying: Drying optimisation. Drying Technology, 18(7), 1433–1448. (2000) https://doi.org/10.1080/07373930008917786
32. Penttilä, P.A., Paajanen, A., Ketoja, J.A.: Combining scattering analysis and atomistic simulation of wood-water interactions. Carbohydrate Polymers, 251, 117064. (2021) https://doi.org/10.1016/j.carbpol.2020.117064.
33. Rajendran, K.: Effect of moisture content on lignocellulosic power generation: Energy, economic and environmental impacts. Processes, 5(4), 78. (2017). https://doi.org/10.33 90/pr5040078.
34. Remond, R., Perré, P., Mougel, E.: Using the concept of thin dry layer to explain the evolution of thickness, temperature, and moisture content during convective drying of Norway spruce boards. Drying technology, 23(1–2), pp.249–271. (2005) https://doi/abs/10.1081/DRT-200047883.
35. Salin, J.G. : Drying of liquid water in wood as influenced by the capillary fiber network. Drying Technology, 26(5), pp.560–567. (2008) https://doi.org/10.1080/07373930801944747
36. Sander, A., Kardum, J.P., Skansi, D.: Transport properties in drying of solids. Chemical and Biochemical Engineering Quarterly 15 (3):131–38. (2001)
37. Saxena, G., Gaur, M.K., Kushwah,A.: Performance Analysis and ANN Modelling of Apple Drying in ETSC-Assisted Hybrid Active Dryer. In Artificial Intelligence and Sustainable Computing (pp. 275–294). (2022) Springer,Singapore. https://doi:10.1007/978-981-16-1220-6_24
38. Soni, S.K.: A source of energy for 21st century. New Delhi: New India Pub. (2007)
39. Thyavihalli, Girijappa, Y.G., Mavinkere, Rangappa, S., Parameswaranpillai, J., Siengchin, S.: Natural fibers as sustainable and renewable resource for development of eco-friendly composites : a comprehensive review. Frontiers in Materials, 226. (2019) https://doi:10.3389/fmats. 2019.00226.
40. Verma, L.R., Bucklin, R.A., Endan, J.B, Wratten, F.T.: Effects of drying air parameters on rice drying models. Transaction of the ASAE, 28, 296–301. (1985)
41. Vega, A., Fito, P., Andres, A., Lemus, R.: Mathematical modeling of ´ hot-air drying kinetics of red bell pepper (var. Lamuyo). J Food Engr 79: 1460–6. (2007) https://doi.org/10.1016/j.jfoodeng. 2006.04.028.

42. Wang, S., Zhang, Y., Xing, C.: Effect of drying method on the surface wettability of wood strands. Holz als Roh-und Werkstoff, 65(6), 437–442. (2007) https://doi.org/10.1007/s00107-007-0191-7.
43. Wang, C.Y., Singh, R.P.: A Single Layer Drying Equation for Rough Rice; ASAE Paper No. 3001; ASAE: St. Joseph, MI, USA. (1978)
44. Wiberg, P., Morén, T.J.: Moisture flux determination in wood during drying above fibre saturation point using CT-scanning and digital image processing. Holz als Roh-und Werkstoff, 57(2), pp.137–144. (1999) https://doi.org/10.1007/s001070050029.
45. Younis, M., Abdelkarim, D., El-Abdein, A.Z.: Kinetics and mathematical modeling of infrared thin-layer drying of garlic slices. Saudi journal of biological sciences. 25(2):332–8. (2018) https://doi.org/10.1016/j.sjbs.2017.06.011
46. Zarea, Hosseinabadi, H., Doosthoseini, K., Layeghi, M.: Drying kinetics of poplar (Populus deltoides) wood particles by a convective thin layer dryer. Drvna industrija, 63(3), 169–176. (2012) https://doi.org/10.5552/drind.2012.1201.
47. Zhao, D., Zhu, Y., Cheng, W., Chen, W., Wu, Y., Yu, H.: Cellulose-based flexible functional materials for emerging intelligent electronics. Advanced materials, 33(28), (2021) 2000619. https://doi.org/10.1002/adma.202000619.
48. Zitting, A., Paajanen, A., Rautkari, L., Penttilä, P.A .: Deswelling of microfibril bundles in drying wood studied by small-angle neutron scattering and molecular dynamics. Cellulose, 28(17), 10765–10776. (2021) https://doi.org/10.1007/s10570-021-04204-y.

Tables

Table 1. Mathematical models applied to drying curves.

Model name	Model equation	Reference
Lewis (Newton)	$MR = \exp(-kt)$	Ghazanfari et al,2006
Henderson and Pabis	$MR = a \exp(-kt)$	Kaur and Singh, 2014
Logarithmic	$MR = a \exp(-kt) + c$	Gan PL and Poh, 2104
Modified Midilli et al.-III	$MR = a \exp(-kt) + ct$	Kaur and Singh ,2014
Two-term	$MR = a \exp(-k_1 t) + b \exp(-k_2 t)$	Kumar et al., 2014
Noomhorm and Verma	$MR = a \exp(-k_1 t) + b \exp(-k_2 t) + c$	Kaleta and Gornicki 2010
Modified Henderson and Pabis	$MR = a \exp(-k_1 t) + b \exp(-k_2 t) + c \exp(-k_3 t)$	Erbay and Icier, 2009
Two-term exponentia	$MR = a \exp(-kt) + (1 - a) \exp(-akt)$	Lee and Kim, 2009
Modified two term-V	$MR = a \exp(-kt) + (1 - a) \exp(-gt)$	Verma et al.1985
Page	$MR = \exp(-kt^n)$	Doymaz, 2007a
Modified Page-IV	$MR = a \exp(-kt^n)$	Babalis et al., 2006
Hii et al	$MR = a \exp(-kt^n) + b \exp(-gt^n)$	Hii et al., 2009
Kaleta et al. II	$MR = a \exp(-kt^n) + (1 - a)\exp(-gt^n)$	Kaleta et al 2013
Modified Page II	$MR = \exp[-(kt)^n]$	Vega et al, 2007
Modified page .III	$MR = a \exp[-(kt)^n]$	Ertekin and Firat 2017
Demir et al.	$MR = a \exp[-(kt)^n] + b$	Demir et al 2007
Wang and Singh	$MR = 1 + at + bt^2$	Wang and Singh 1978
Midilli et al.	$MR = a \exp(-kt^n) + bt$	Midilli et al., 2002

Table 2. Statistical results and drying constant of mathematical models at different temperature drying. (T=105 C).

T	Model	R^2	Constant Parameters	RSME	SSE
105	F(t) = exp(-kt)	0.522	k =0.001095	0.3785	17.91
	F(t) = a exp(-kt)	0.986	a =2.004, k =0.002016	0.06489	0.5221
	F(t)=a exp(-kt) +c	0.9991	a =2.352, k =0.00129, c = -0.4487	0.01638	0.03298
	F(t)=a exp(-kt) +c t	0.999	a = 1.909, k =0.001517, c = -0.0002181	0.01715	0.03619
	F(t)=a exp(-k_1t) +c exp(-k_2t)	0.9991	a =58.78, k_1 =0.0007727, k_2 =0.0007472, c =-56.89	0.01646	0.03304
	F(t)=a exp(-k_1t) +b exp(-k_2t) +c	0.9991	a=2.361, k_1 =0.00126, k_2 =0.01683, c =0.02563, d =-0.471	0.01627	0.03205
	F(t)=a exp(-k_1t) +c exp(-k_2t) +d exp(-k_3t)	0.9981	a =20.62, k_1 = 0.0002808, k_1 = 0.003502, k_3 = 0.0002256 c =0.5778, d =-19.28	0.02422	0.07037
	F(t)=a exp(-k_1t) +(1-a) exp(-ak_2t)	0.5598	a =18.57, k_1 =0.0003812, k_2 =1.902e-05	0.3655	16.43
	F(t)=a exp(-kt) +(1-a) exp(-gt)	0.9229	a =2.035, k =0.002048, g = 0.9649	0.153	2.878
	F(t)=exp(-kt^n)	0.991	k= 2.326e-08, n =2.617	0.05198	0.335
	F(t)=a exp(-kt^n)	0.9955	a =1.827, k =0.0002737, n =1.298	0.03695	0.1679
	F(t)=a exp(-kt^n) +(1-a) exp(-gt^n)	0.9317	a =1.787, k =0.0001936, g = 0.9649, n =1.348	0.1445	2.548
	F(t)=a exp(-kt^n) +bt	0.9993	a =1.571, k =7.104, c =-0.001415, n = -9.327	0.02559	0.02934
	F(t)=1+at+bt^2	0.6887	a = 0.00017, b = -9.287e-07	0.3061	11.62
	F(t)=a exp[-$(kt)^n$]	0.9955	a =1.827, k =0.001797, n =1.298	0.03695	0.1679
	F(t)= exp[-$(kt)^n$]	0.7135	k = 0.001215, n = 3.284	0.2925	10.61
	F(t)=a exp[-$(kt)^n$] +b	0.9991	a =2.359, k =0.001285, c =-0.4543, n =0.9974	0.02644	0.03298

Table 3. Statistical results and drying constant of mathematical models at different temperature drying. (T=120 C).

T		R	CONSTANT	RSME	SSE
120	f(t) = exp(-kt)	0.5283	k =0.001879	0.3961	10.2
	f(t) = a exp(-kt)	0.9834	a =2.03, k = 0.004077	0.07483	0.3584
	F(t)=a exp(-kt) +c	0.9953	a =2.33, k =0.002757, c =-0.3846	0.0395	0.0183
	F(t)=a exp(-kt)+ct	0.9951	a = 1.95, k = 0.003183, c = -0.000384	0.04088	0.1053
	F(t)=a exp($-k_1$t) +c exp($-k_2$t)	0.9956	a =-21.48, k_1 =0.001749, k_2 = 0.001879, c = 23.44	0.03921	0.01533
	F(t)=a exp($-k_1$t) +c exp($-k_2$t) +d	0.9955	a =0.02299, k_1 =1.886, k_2 = 0.002709 c = 2.335, d =-0.3999	0.03996	0.09742
	F(t)=a exp($-k_1$t) +c exp($-k_2$t) +d exp($-k_3$t)	0.9896	a = -0.1399, k_1 =0.003085, k_2 = -7.165e-05, k_3= 0.0022, c =-0.5655, d =2.515	0.06121	0.2248
	F(t)=a exp($-k_1$t) +(1-a) exp($-ak_2$t)	0.5332	a=10.8, k_1= 0.001431, k_2 =0.0001278	0.4003	10.09
	F(t)=a exp(-kt) +(1-a) exp(-gt)	0.6409	a =23.93, k = -0.001424, g = -0.001497	0.3511	7.766
	F(t)=exp($-kt^n$)	0.6957	k =1.629e-08, n =2.979	0.3207	6.581
	F(t)=a exp($-kt^n$)	0.9938	a = 1.866, k = 0.0006577, n = 1.305	0.0462	0.1345
	F(t)=a exp($-kt^n$)+(1-a)exp($-gt^n$)	0.5595	a =0.5306, k = 0.0008578, g = 0.0008555, n = 1.137	0.392	9.525
	F(t)=a exp($-kt^n$) + bt	0.9993	a =1.683, k =-0.0001672, c =-0.005202, n = 1.289	0.03104	0.010839
	F(t)=1+at+bt^2	0.6606	a = 0.0001447, b = -3.198e-06	0.3387	7.34
	F(t)=a exp[$-(kt)^n$]	0.9938	a =1.866, k = 0.003653, n =1.305	0.0462	0.1345
	F(t)= exp[$-(kt)^n$]	0.6966	k =0.002446, n = 3.258	0.3202	6.562
	F(t)=a exp[$-(kt)^n$] +c	0.9957	a =2.163, k =0.003044, c = -0.2463, n =1.088	0.03875	0.09308

Table 4. Statistical results and drying constant of mathematical models at different temperature drying. (T=135 C).

T		R	CONSTANT	RSME	SSE
135	$F(t) = \exp(-kt)$	0.5162	k =0.003319	0.4435	8.064
	$F(t) = a \exp(-kt)$	0.9779	a =2.105, k =0.007026	0.09605	0.369
	$F(t)=a \exp(-kt) +c$	0.9955	a =2.466, k =0.004556, c = -0.4479	0.04369	0.07445
	$F(t)=a \exp(-kt) +ct$	0.9948	a = 2.023, k = 0.00535, c = -0.0007366	0.04732	0.08732
	$F(t)=a \exp(-k_1t)+c \exp(-k_2t)$	0.9899	a =156.1, k_1=0.0134, k_2 = 0.01358, c = -154.3	0.06657	0.1684
	$F(t)=a \exp(-k_1t) +c \exp(-k_2t) +d$	0.9923	a = 42.25, k_1 = 0.01385, k_2 = 0.01444, c = -40.38, d = 0.08261	0.05903	0.1289
	$F(t)=a \exp(-k_1t) +c \exp(-k_2t) +d \exp(-k_3t)$	0.9969	a =20.54, k_1 = 0.01244, k_2 = 0.01039, k_3 = 0.01324, c = 1.814, d =-20.37	0.03795	0.05183
	$F(t)=a \exp(-k_1t) +(1-a) \exp(-ak_2t)$	0.5242	a =19.77, k_1 =0.002262 k_2 = 0.0001113	0.4507	7.921
	$F(t)=a \exp(-kt) +(1-a) \exp(-gt)$	0.8228	a =2.306, k =0.007674, g =0.9575	0.2752	2.953
	$F(t)=\exp(-kt^n)$	0.6787	k =2.107e-08, n = 3.226	0.3659	5.356
	$F(t)=a \exp(-kt^n)$	0.9985	a = 1.92, k = 0.0006959, n =1.43	0.02557	0.0255
	$F(t)=a \exp(-kt^n) +(1-a) \exp(-gt^n)$	0.835	a = 1.831, k = 0.0003666, g = 0.8876, n =1.543	0.269	2.75
	$F(t)=a \exp(-kt^n) +bt$	0.9992	a = 1.938, k =0.001101, c = -0.0001875, n = 1.33	0.01871	0.0113
	$F(t)=1+at+bt^2$	0.6357	a = 3.394e-05, b = -8.057e-06	0.3896	6.072
	$F(t)=a \exp[-(kt)^n]$	0.9985	a = 1.92, k =0.006198, n =1.43	0.02557	0.0255
	$F(t)= \exp[-(kt)^n]$	0.6794	k =0.004207, n = 3.565	0.3655	5.343
	$F(t)=a \exp[-(kt)^n] +c$	0.9992	a =2.031, k =0.005811, c = -0.09174, n =1.313	0.01848	0.01298

Table. 5. Evaluation the performance of neural network using statistical parameters

Factor	Parameter	R	MSE	MAPE
	training	0.99998	**0.000011**	
MC	validation	0.99998	**0.000014**	
	testing	0.99993	**0.00005**	
	All data	**0.99997**		2.53

Figures

Figure 1

Moisture Analyzer, MB45 AM (ohaus.com)

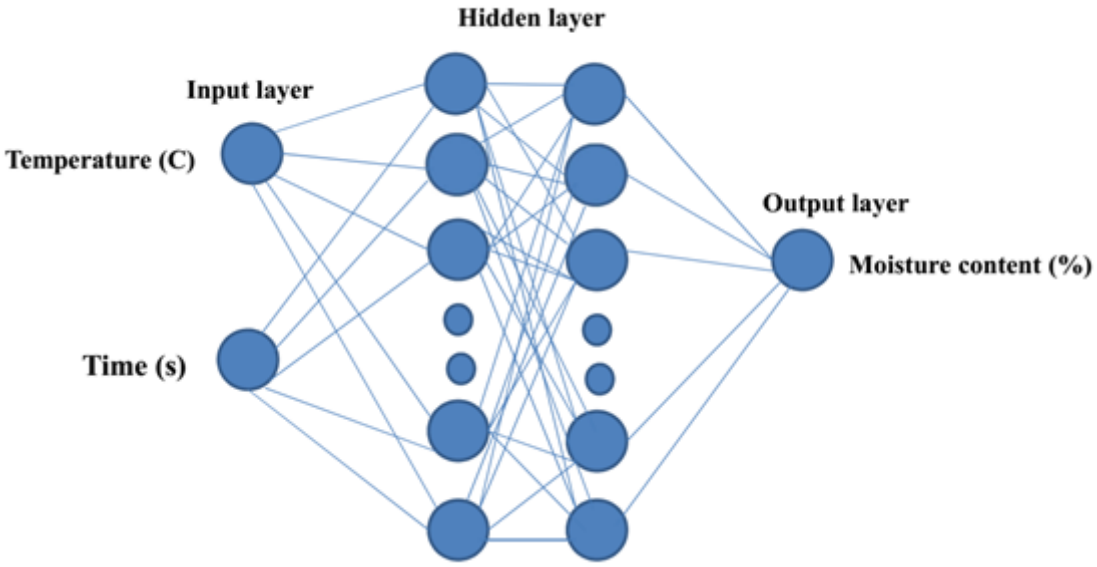

Figure 2

Schema of artificial neural network for prediction moisture content of wood fiber.

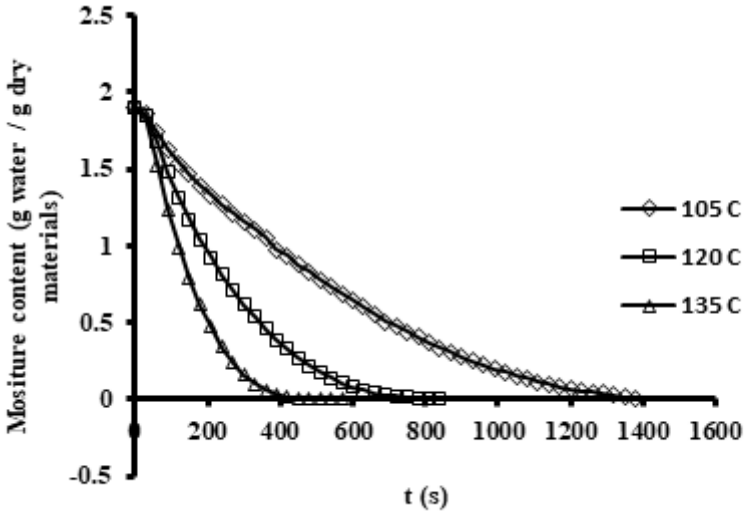

Figure 3

Moisture content versus drying time at different halogen drying temperature.

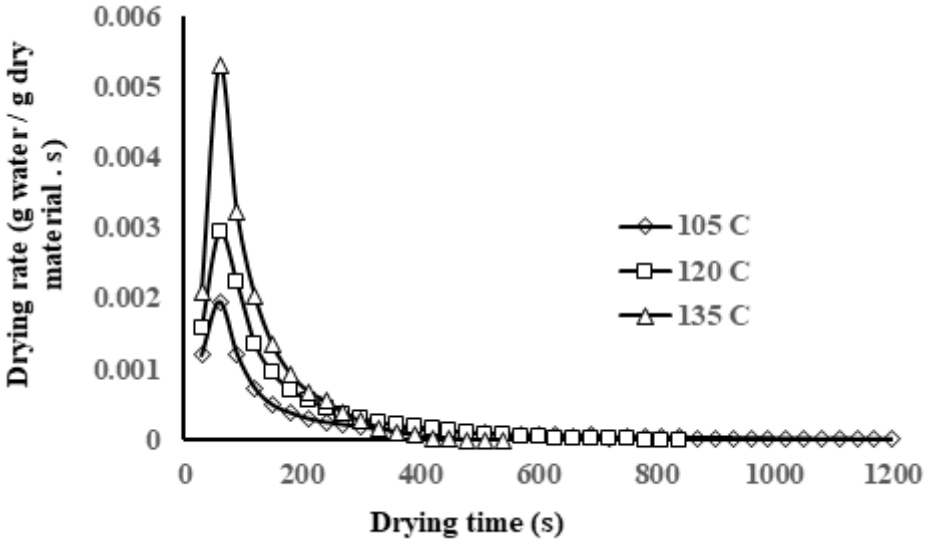

Figure 4

Drying rate versus drying time at different halogen drying temperature.

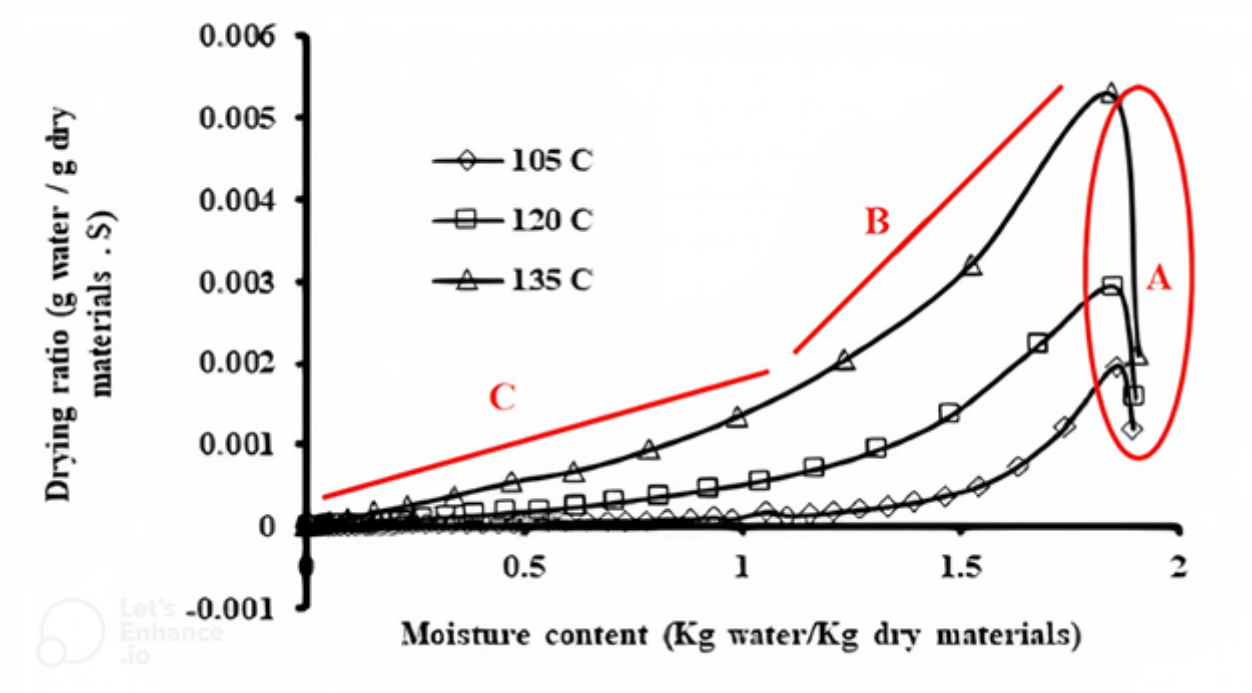

Figure 5

Drying rate versus moisture content at different halogen drying temperature

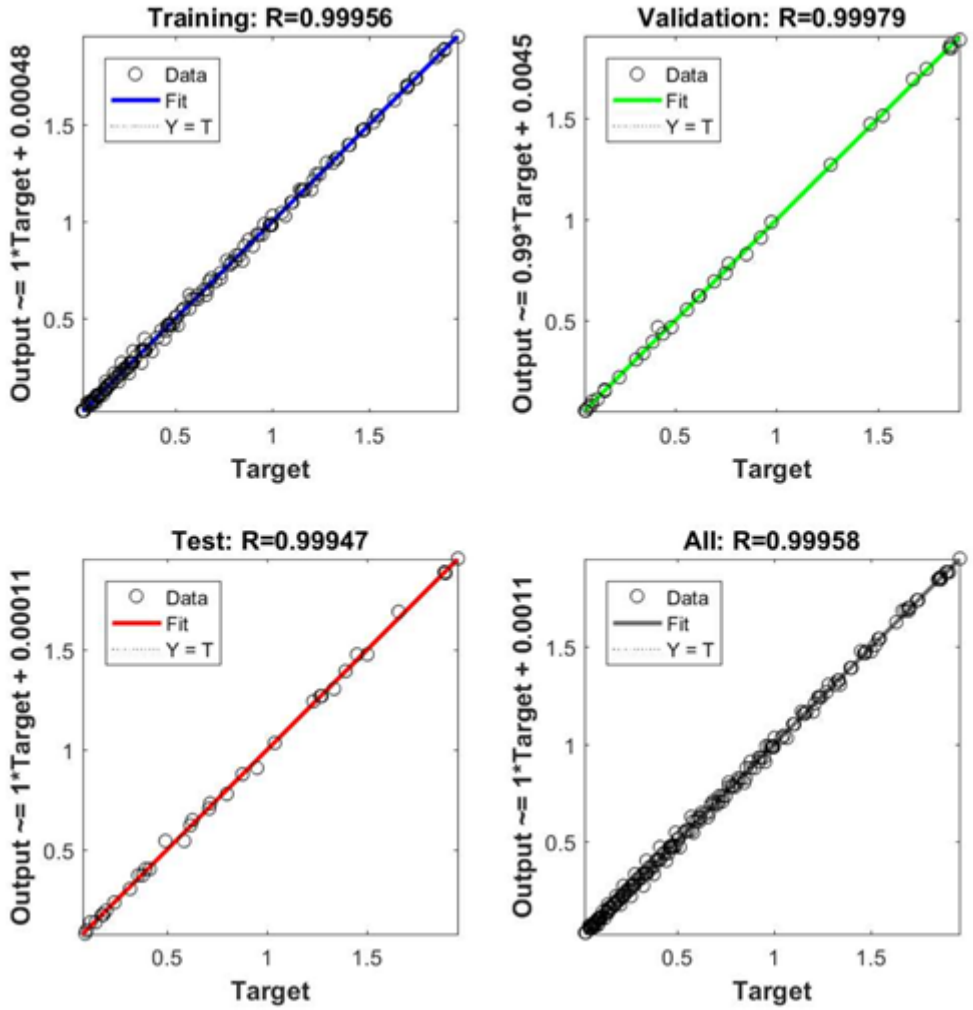

Figure 6

Regression plots of the developed ANN model for (a) the training data set, (b) the validation data set, (c) the testing data set, and (d) All data.

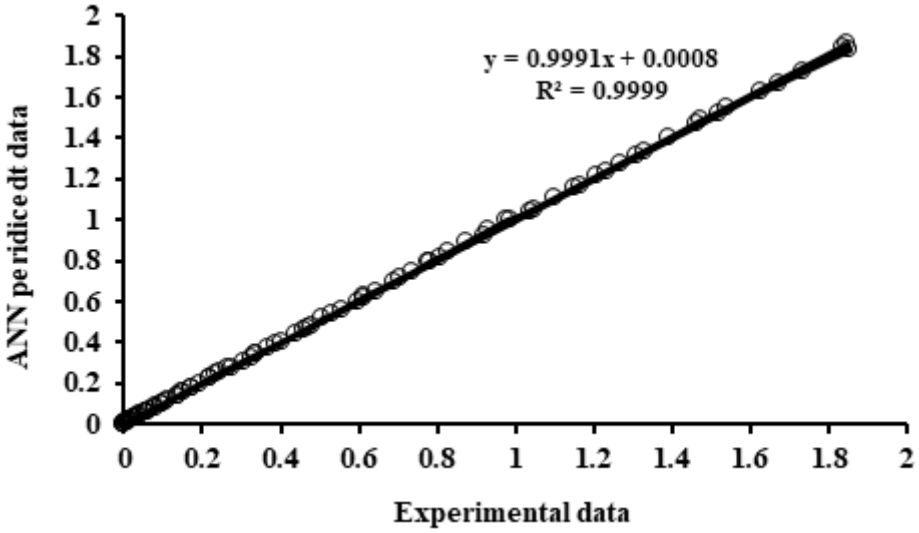

Figure 7

Comparison of ANN predictions and experimental data

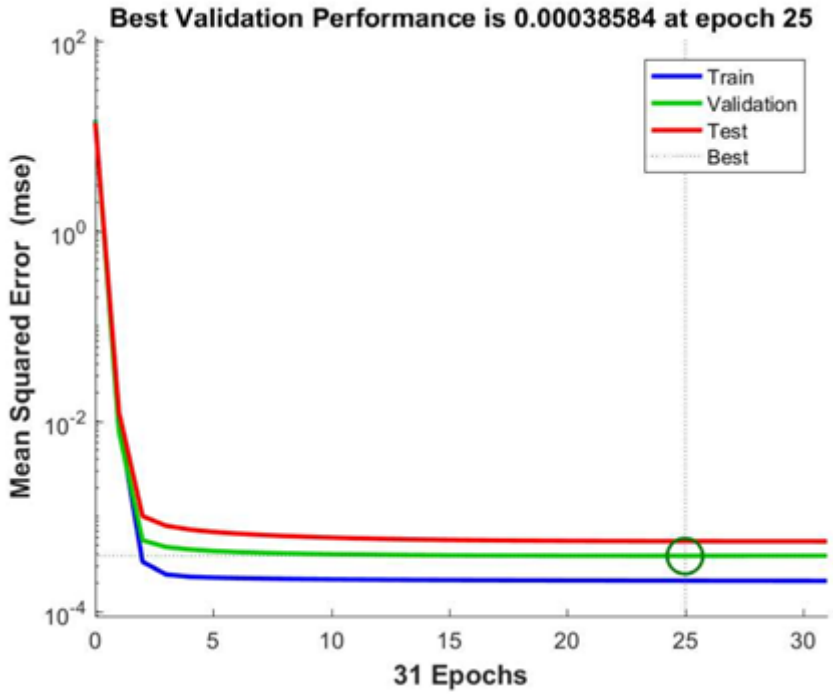

Figure 8

Neural network performance by period (epoch) for training, validation, and testing data.